JPET Fast Forward. Published on October 25, 2011 as DOI: 10.1124/jpet.111.185835
JPET/2011/185835

Title page

Structural Nucleotide Analogs are Potent Activators/Inhibitors of Pancreatic Beta-Cell KATP Channels: an Emerging Mechanism Supporting Their Use as Anti-Diabetic Drugs.

Domenico Tricarico[1], Jean-François Rolland[1], Gianluigi Cannone, Antonietta Mele, Valentina Cippone, Antonio Laghezza, Giuseppe Carbonara, Giuseppe Fracchiolla, Paolo Tortorella, Fulvio Loiodice and Diana Conte Camerino

Department of Pharmacobiology, Faculty of Pharmacy, via Orabona no. 4, University of Bari, I-70126 Bari, Italy(D.T., J-F. R., G.C., A.M., V.C., D.C.C.); Department of Medicinal Chemistry , Faculty of Pharmacy, via Orabona no. 4, University of Bari, I-70126 Bari, Italy (A.L., G.C., G.F. ,P.T., F.L.)

JPET/2011/185835

Running title page

Running title : K^+ channel modulators and pancreatic beta cells

Corresponding author: Domenico Tricarico

address: Dept. of Pharmacobiology, Faculty of Pharmacy, via Orabona n° 4, Bari, Italy

FAX: 00390805442801

phone: 00390805442795

e-mail address: dtricarico@farmbiol.uniba.it

number of words in the introduction: 745

number of words in the discussion: 1270

number of words in the abstract: 240

number of tables: 2

number of figures: 9

number of references: 37

number of text pages: 37

Abbreviations: KCO, potassium channel openers; KATP, ATP-sensitive K^+-channels; DE_{50}, drug concentration needed to enhance the current by 50%; IC_{50}, drug concentration needed to inhibit the current by 50%; IGTT, intraperitoneal glucose tolerance test; i.p., intraperitoneal; AUC, area under the curve; MOPS, 3-(N-morpholino) propane-sulphonic acid; DMSO, dimethylsulphoxide; SUR1, sulfonylureas receptor type-1; Kir6.2, inwardly rectifying K^+channel.

Sections: cellular and molecular; endocrine and diabetes

JPET Fast Forward. Published on October 25, 2011 as DOI: 10.1124/jpet.111.185835
This article has not been copyedited and formatted. The final version may differ from this version.

Abstract

The 2*H*-1,4-benzoxazine derivatives are novel drugs structurally similar to nucleotides; however, their actions on the pancreatic beta-cell ATP-sensitive-K^+(KATP) channel and on glucose disposal are unknown. Therefore, the effects of the linear/branched alkyl substituents and the aliphatic/aromatic rings at position 2 of the 2*H*-1,4-benzoxazine nucleus on the activity of these molecules against the pancreatic beta-cell KATP channel and the Kir6.2ΔC36 subunit were investigated using a patch-clamp technique. The effects of these compounds on glucose disposal that followed glucose loading by i.p. GTT and on fasted glycemia were investigated in normal mice. The 2-*n*-hexyl analog blocked the KATP(IC_{50}=10.1x10^{-9}M) and Kir6.2ΔC36(IC_{50}=9.6x10^{-9}M) channels which induced depolarization. In contrast, the 2-phenyl analog was a potent opener(DE_{50}=0.04x10^{-9}M), which induced hyperpolarization. The ranked order of the potency/efficacy of the analog openers was 2-phenyl>2-benzyl>2-cyclohexylmethyl. The 2-phenylethyl and 2-isopropyl analogs were not effective as blockers/openers. The 2-*n*-hexyl (2-10 mg kg^{-1}) and 2-phenyl analogs (2-30 mg kg^{-1}) reduced and enhanced the glucose AUC curves, respectively, following the glucose loading in mice. These compounds did not affect the fasted glycemia as is observed with glibenclamide. The linear alkyl chain and the aromatic ring at position 2 of the 1,4-benzoxazine nucleus are the determinants, which respectively confer the KATP channel blocking action with glucose lowering effects and the opening action with increased glucose levels. The opening/blocking actions of these compounds mimic those that were observed with ATP and ADP. The results support the use of these compounds as novel anti-diabetic drugs.

JPET Fast Forward. Published on October 25, 2011 as DOI: 10.1124/jpet.111.185835
This article has not been copyedited and formatted. The final version may differ from this version.

Introduction

Drugs that target the pancreatic beta-cell ATP-sensitive-K^+(KATP) channels are used in the glucose/insulin dis-metabolisms(Gribble and Reimann, 2003; Jahangir and Terzic, 2005; Ashcroft, 2010; Arnoux et al., 2010). This channel is a complex that is composed of the sulfonylureas receptor type-1(SUR1) and the inwardly rectifying K^+channel(Kir6.2) subunits(Seino and Mikia, 2003). The SUR1 subunit carries the binding sites for the KATP channel openers and blockers (Babenko et al., 2000; Moreau et al., 2005). KATP channel blockers are prescribed to individuals who are in the diabetic-aged population and who display impaired glucose-induced insulin release (Nourparvar et al., 2004). These drugs belong to the following distinct classes: the first generation sulfonylureas (chlorpropamide, tolbutamide and tolazamide), which are low affinity ligands of the SUR1 subunit that exert the release of insulin at micromolar concentrations; the second (glipizide and glyburide) and third (glimiperide and acetohexamide) generation sulfonylureas, which are the high affinity and slowly reversible ligands of the SUR1 subunit that act at nanomolar concentrations; and the glinides, which lack the sulfonylurea moiety and include repaglinide, nateglinide and meglitinide, which are high affinity SUR1 ligands, exhibit a rapid onset/offset action when compared to that of the sulfonylureas(Gribble and Reimann, 2003).

The sulfonylureas and the glinides are being investigated for their uses in the treatment of hypotension that results from septic shock, ischemic trauma and neonatal diabetes(Koster et al., 2005; Flechtner et al., 2006; Pearson et al., 2006; Mlynarski et al., 2007; Flanagan et al., 2007; Simard et al., 2008; Ashcroft, 2010). Severe hypoglycemia, weight gain and cardiovascular side effects limit their use in the special populations(Zünkler, 2006). The long-term exposure of the beta-cells to sulfonylureas induces a reduction in the insulin content and of the number of KATP channels(Takahashi et al., 2007). Therapeutic concentrations of sulfonylureas and high doses of glinides induce the apoptosis of beta cells, beta-cell lines or cell lines that express the recombinant KATP channel subunits, and these effects are mediated by SUR1(Maedler et al., 2005; Hambrock et

al., 2006). Glibenclamide also causes atrophy of the skeletal muscles (Tricarico et al., 2010). It has been proposed that sulfonylurea-induced atrophy contributes to the loss of beta-cell mass that characterizes the progression of diabetes (Takahashi et al., 2007).

The pancreatic KATP channel openers(KCO) belong to the benzothiadiazine, which includes the diazoxide and thiadiazine-1,1-dioxide derivatives, such as BPDZ-62, BPDZ-73, NNC-55-0462, NNC-55-0118 and NN414; cyanoguanidines; nitropyrazoles; and 4-sulfamoylphenylbenzamides(Hansen, 2006; Carosati et al., 2007). Diazoxide is prescribed for the treatment of acquired and tumor-related hypoglycemia, familial hyperinsulinemia hypoglycemia in infancy and polycystic ovary syndrome(Jahangir and Terzic, 2005; Hussain, 2007; Arnoux, 2010). Diazoxide protects the beta-cells from sulfonylurea-induced apoptosis, high glucose and cytokine-induced toxicity, which preserves the insulin stores(Teshima et al., 2003). In skeletal muscle, diazoxide prevents glibenclamide-induced atrophy(Tricarico et al., 2010). The SUR1-selective openers have been proposed to treat epilepsy and neurodegenerative disorders, in which the SUR1/Kir6.2-Kir6.1 subunits play a role(Carosati et al., 2007). However, diazoxide is unselective, which can lead to hypotension and tachycardia, severe fluid retention, sedation and weakness.

The 2*H*-1,4-benzoxazine derivatives have emerged as novel KATP channel modulators. In the presence of ATP, these molecules display KCO activity, while in the absence of nucleotide, they display a blocking action(Tricarico et al., 2003; 2008). These compounds have structural similarities with ATP and ADP molecules. A conformational analysis showed that the planar area of the 2*H*-1,4-benzoxazines overlaps with that of the adenine nucleotide tri- and diphosphates. The electronic distribution profile of this area is also similar with that of the adenine nucleotides, which were reached by electrons; this result suggests that these compounds share a common ATP/ADP interaction interface on the receptor sites(Tricarico et al., 2008). No data are available regarding the

effects or possible dualistic actions of these nucleotide analogs on the pancreatic beta-cell KATP channel or glucose disposal in normal mice.

The molecular determinants that were responsible for the activity of the 2*H*-1,4 benzoxazine derivatives toward the beta-cell KATP channels and the Kir6.2ΔC36 subunit that was expressed in HEK293 cells were therefore investigated using patch-clamp techniques. The influence of the linear/branched alkyl chain substituents at position 2 of the 2*H*-1,4-benzoxazine nucleus on the biological activity of the molecules against the KATP channel was evaluated by testing the effects of the 2-*n*-hexyl and 2-isopropyl-1,4-benzoxazine derivatives. The influence of an aromatic/aliphatic ring on the biological activity of the molecules against the KATP channels was evaluated by testing the effects of 2-cyclohexylmethyl, 2-phenyl, 2-benzyl and 2-phenylethyl-1,4-benzoxazines(Fig. 1). The drug effects on glucose disposal and on fasted glycemia in normal mice were also investigated.

Methods

Pancreatic beta cells and tsA201 cells expressing the Kir6.2ΔC36 channel. All of the experiments were conducted in accordance with the Italian Guidelines for the use of laboratory animals, which conforms with the European Community Directive that was published in 1986 (86-609-EEC). The method of pancreatic beta-cell preparation has been previously described (Rolland et al., 2002, Rolland et al., 2006). Sixty to one hundred islets per culture from 2 mice were prepared. The islets were identified by optical morphological inspection and insulin secretion. The beta cells were identified by their spherical form/size, capacitance of 8±3 pF (number of cells=45) (alpha or delta cells have a lower capacitance), current/membrane potential response to high or low glucose concentrations (see step 1 below), current responses to diazoxide or tolbutamide (see step 5 below) and insulin secretion in response to increasing concentrations of external glucose (Fig. 2A, B, C). Studies on the Kir6.2ΔC36 channel in HEK293 cells utilized Kir6.2ΔC36 (mouse) that was

JPET Fast Forward. Published on October 25, 2011 as DOI: 10.1124/jpet.111.185835
This article has not been copyedited and formatted. The final version may differ from this version.

inserted in the mammalian expression vector pCDNA3, which was generously provided by Professor FM Ashcroft. The HEK293 cells were co-transfected with 4 μg of DNA that encoded the channel and a lower amount of plasmid DNA that encoded the CD8 receptors using Lipofectamine 2000 and Opti-MEM (Invitrogen, U.S.A.).

Insulin secretion. Triplicates of the 8 islets were cultured in 10% fetal calf serum and 1 ml Krebs-Ringer bicarbonate buffer with HEPES (KRBH) medium with 2 mg/ml BSA and 5 mmol/l glucose overnight in air (5% CO_2) at 37°C before the experiments. An equilibrium period of 120 min in 0 mM glucose of the islets was performed; this was followed by a period of incubation with different glucose concentrations (0.5-10 mM) for 60 min in 5% CO2 at 37°C to evaluate the insulin secretion in the medium. The islets were sonicated to facilitate insulin extraction. The insulin concentration in the sonicate and the medium was determined with the use of rat/mouse insulin ELISA (Millipore Co., MA) (Fig. 2C).

Solutions and drugs. For the perforated or conventional whole-cell recordings, the extracellular bath solution contained (in mM) 140 NaCl, 4.8 KCl, 2.5 $CaCl_2$, 1.2 $MgCl_2$, 10 HEPES (pH 7.4), and various concentrations of glucose. The electrical contact was established by adding amphotericin-B to the pipette solution (stock: 60 mg ml^{-1} in DMSO, final concentration: 300 μg ml^{-1}). For the perforated patch mode, the pipette solution contained (in mM) 70 K_2SO_4, 10 NaCl, 10 KCl, 3.7 $MgCl_2$ and 5 HEPES (pH=7.1); 5 K_2ATP and 1 Na_3GTP were added to the pipette solution for the conventional whole-cell mode. K_2SO_4 was replaced by an equimolar concentration of KCl using $BaCl_2$. For the inside-out recordings, the bath solution contained (in mM) 140 KCl, 5 mM EGTA and 20 HEPES (pH=7.2). The intrapipette solution contained (in mM) 140 KCl, 2.6 $CaCl_2$, 1 $MgCl_2$, 10 EGTA and 20 HEPES (pH =7.4). The synthesis of the 2*H*-1,4-benzoxazine derivatives has been previously described (Fig. 1) (Tricarico et al., 2003). All of the other chemicals were purchased from Sigma (Milano, Italy).

JPET Fast Forward. Published on October 25, 2011 as DOI: 10.1124/jpet.111.185835
This article has not been copyedited and formatted. The final version may differ from this version.

Patch clamp experiments. The drug experiments were performed using the patch-clamp methodology in the voltage-clamp mode (perforated whole-cell, conventional whole-cell and inside-out configurations) and the current-clamp mode was performed using Clampex software (Axon Instruments, Union City, CA) (Tricarico et al., 2008, Rolland et al., 2006).

The pancreatic beta cells were continuously perfused with different solutions at the flow rate of 2 ml min^{-1}, and the changes in the currents were monitored. The patch perforation and whole-cell configurations were evaluated by monitoring the changes in the current capacitance and access resistance which were 22±6 MΩ and 30±3 MΩ in the whole-cell and perforated patch experiments, respectively. The protocol that was applied for the identification of beta cells and the drug test was as follows:

1) external glucose 10 mM, 6 mM or 3 mM+NaN_3 (5 mM)

2) external glucose 10 mM, 6 mM or 3 mM+NaN_3 (5 mM) (control)

3) external glucose 10 mM, 6 mM or 3 mM+NaN_3 (5 mM)+drugs

4) washout

5) external glucose 10 mM, 6 mM or 3 mM/NaN_3 (5 mM)+diazoxide ($2.5x10^{-4}$M) or tolbutamide ($5x10^{-4}$M)

No more than 2 drug concentrations per cell were tested. The drug solutions were applied to the patches using a fast perfusion system (AutoMate, Sci. U.S.A.).

It should be noted that the low patch-clamp performance in 10 mM glucose can mask the blocking actions of the investigated drugs. In this experimental condition, we indeed measured a very low residual current that did not allow us to quantify the blocking action of the drugs on this parameter.

JPET Fast Forward. Published on October 25, 2011 as DOI: 10.1124/jpet.111.185835
This article has not been copyedited and formatted. The final version may differ from this version.

Intraperitoneal glucose tolerance test (IGTT). This test was performed on 6 groups of 8-week-old non-diabetic mice following an overnight fast as previously described (Rolland et al., 2006). The non-cyclic 2*H*-1,4-benzoxazine derivatives (0.2, 2, 10 or 30 mg kg^{-1}), the 2-phenyl analog (2, 10 and 30 mg kg^{-1}), glibenclamide (0.2, 2 mg kg^{-1}) and diazoxide (2 mg kg^{-1}) were dissolved in a solution that contained polyoxyethylenesorbitan-monooleate (10%) and 0.9% NaCl (90%).

This treatment was followed with evaluations at 24 hrs and 14 days post-dose to identify any possible intolerability of the single i.p. injection of the compounds. The primary endpoints that were evaluated were mild symptoms, such as piloerection, sedation and weakness. The secondary endpoints were severe symptoms such as abdominal cramps, convulsion and moribundity.

Analysis of the results and statistics. The off-line analysis was performed using Clampfit, Fetchan, pSTAT (Axon Instruments), and Microsoft Excel (Microsoft, Redmond, WA). The mean current (single channel current x open probability x number of channels) was evaluated in an excised-patch as the digital average of the sampled points, while the single channel conductance (pS) was evaluated as the slope of the current-voltage relationship. The experiments are illustrated by the traces, means or representative results that were obtained from at least 3 different cultures. The concentration-response data were fitted by an equation that described the interaction of the ligand with one inhibitory site, as in the case of the 2-hexyl analog data, or by the sum of two equations that described the interaction of the ligand with two sites that exerted opposite actions, as in the case of the 2-cyclic analog data (Tricarico et al., 2008). The stimulatory component can be described by the following term:

$$(I\ drug\text{-}1)x100=Amax/(1+ (DE_{50}/[Drug])^{n}),$$

and the inhibitory component can be described by the following term:

$$(I\ drug\text{-}1)x100=Imax/(1+ ([Drug]/IC_{50})^{n}.$$

JPET Fast Forward. Published on October 25, 2011 as DOI: 10.1124/jpet.111.185835
This article has not been copyedited and formatted. The final version may differ from this version.

I max indicates the percentage maximal inhibition of the pancreatic KATP channel and Kir6.2ΔC36 channel currents that were caused by the compounds. A max indicates the percentage maximal activation of the KATP currents that was produced by the compound under investigation. DE_{50} indicates the concentration of the drug that was needed to enhance the current by 50%, which was calculated with respect to the current levels that were recorded in the absence of drugs. IC_{50} is the concentration of the drug that is needed to reduce the current by 50%, which was calculated with respect to the current levels that were recorded in the absence of the drugs. N indicates the number of sampled cells per drug, while, *n* indicates the slope factor of the curves. The algorithms of the fitting procedures that were used were based on a Marquardt least-squares fitting routine. The data analysis and the plot were performed using SigmaPlot software (Systat Software, Inc., San Jose, CA). The data are expressed as the means$\pm$S.E. The statistical significance of the differences between the means was assessed by the Student's t-test. The differences were considered significant for $P<0.05$.

Results

Effects of 2H-1,4-benzoxazine derivatives on the native pancreatic beta-cell KATP channels of mice and on the Kir6.2ΔC36 channel that was expressed in HEK293 cells. We first evaluated the effects of 2-isopropyl and 2-*n*-hexyl analogs on the beta-cell KATP channel in the presence of a 3, 6 or 10 mM concentration of glucose in the bath using the perforated and/or conventional whole-cell patch clamp mode. The exposure of the patches to a solution that was enriched with the 2-linear alkyl chain analog (10^{-10} M-10^{-4} M) inhibited the KATP channel currents of beta cells in the perforated and conventional whole-cell mode in a concentration-dependent manner (Fig. 3A, B, F). In the perforated whole cell patch mode, at -50 mV (Vm) the current was reduced from 42$\pm$3 pA in the control to 18$\pm$3 pA following the application of a 10^{-7} M concentration of the drug (Fig. 3A). In the conventional whole cell mode, at -50 mV (Vm) the current was reduced from 38$\pm$2 pA in the control to 25$\pm$2 pA and 19$\pm$3 pA following the

JPET Fast Forward. Published on October 25, 2011 as DOI: 10.1124/jpet.111.185835
This article has not been copyedited and formatted. The final version may differ from this version.

application of 10^{-8} M and 10^{-7}M concentrations of the drug, respectively(Fig 3B). In the intact cell, the inhibitory effect of this compound was fully reversible after a 5 sec washout of the drug solution. The 2-*n*-hexyl analog (from 10^{-10} M to 10^{-4} M) reduced the Kir6.2ΔC36 channel currents that were recorded in the HEK293 cells pulsed to a test potential of –100 mV (Vm) using the conventional whole-cell patch mode. This drug reduced the Kir6.2ΔC36 current from -980 pA±22 pA in the control to 750±36 pA and 200±21 pA in the presence of 10^{-8}M and 10^{-6} M concentrations of the drug, respectively(Fig. 3C). In the presence of 6 mM glucose, in the perforated patch mode the current was reduced from 21±3 pA in the control to 10±2 pA following application of a 10^{-7}M concentration of the blocker (Fig. 3D). In the perforated patch mode, the 2-branched alkyl chain analog failed to affect the KATP currents either in the presence of 3 mM glucose and 5 mM NaN_3 or 6 mM glucose (Fig. 3A, D), and it did not affect the Kir6.2ΔC36 channel. In the presence of 10 mM glucose, the 2-*n*-hexyl- and 2-isopropyl analogs (10^{-8}M-10^{-6} M) did not significantly affect the currents (Fig. 3E). A $5x10^{-4}$M concentration of tolbutamide almost fully reduced the currents in 3 mM and 6 mM glucose, and it showed a mild effect in 10 mM glucose (Fig. 3A, D, E). The mild blocking effect of tolbutamide that was observed in 10 mM glucose may be related to the low patch-clamp performance that was described in Materials and Methods.

The concentration-response curve analysis showed that at -50 mV (Vm), in 3 mM glucose and using perforated patch method, the IC_{50} of the 2-hexyl analog that was present in the range of concentrations tested was $10.1±3x10^{-9}$M; in the conventional whole-cell patch mode, the IC_{50} was $9.8±2x10^{-9}$M in the beta cells and $9.6±1 x10^{-9}$M in the cell line that was expressing the Kir6.2ΔC36 channel (Fig. 3F; Table 1). These values were not statistically different.

The co-application of 10^{-9}M glibenclamide and the 2-*n*-hexyl analog (10^{-8}M) to the beta cells caused a 53±4% reduction in the currents (number of cells=3) in the conventional whole-cell patch mode. Glibenclamide (10^{-9}M) and the 2-*n*-hexyl analog (10^{-8}M) caused a 25±3% (number of cells=2) and 27±4% (number of cells=3) reduction in the currents, respectively. The KATP current

JPET Fast Forward. Published on October 25, 2011 as DOI: 10.1124/jpet.111.185835
This article has not been copyedited and formatted. The final version may differ from this version.

was indeed reduced from 39±2 pA in the control to 29±2 pA in the presence of 10^{-9}M glibenclamide and 16±2 pA following the co-application of 10^{-9}M glibenclamide and 10^{-8}M of the 2-*n*-hexyl analog to the cell (Fig 3B).

Conversely, in the perforated patch-clamp experiment and in the presence of 3 mM or 6 mM external glucose, the 2-phenyl-, 2-benzyl- and 2-cyclohexylmethyl-1,4-benzoxazine derivatives enhanced the KATP currents at sub-nanomolar concentrations. In 3 mM glucose and 5 mM NaN_3, the percentage activation of the currents was 91.2±4% (number of cells=12) and 58.2±6% (number of cells=7) for 10^{-10} M of the 2-phenyl and 2-benzyl analogs, respectively. The currents that were measured at -50 mV (Vm) in 3 mM glucose+5 mM NaN_3 were 40 pA±4 in the control and 65±4 pA and 75±5 pA with $0.7x10^{-10}$M and 10^{-10}M concentrations of the 2-phenyl analog, respectively; they were 61±5 pA following the application of a 10^{-10}M concentration of the 2-benzyl analog (Fig. 4A). For the 2-phenyl and 2-benzyl analogs in 6 mM glucose, the activation was 96.1±8% (number of cells=4) and 61.2±6% (number of cells=4), respectively. The currents that were measured at -50 mV (Vm) in 6 mM glucose were 19.5±3 pA in the control and 38±4 pA and 32±4 pA following the application of a 10^{-10} M concentration of the 2-phenyl and 2-benzyl analogs, respectively (Fig. 4B). In 3 mM glucose and 5 mM NaN_3 or 6 mM glucose, 10^{-7}M of the 2-phenyl- analog produced a 17±5% (number of cells=12) and 20±6% (number of cells=3) reduction of the respective currents with respect to the controls, while the 2-benzyl analog produced a 21±4% (number of cells=7) and 16±5% (number of cells=4) increase in the currents, respectively (Fig. 4A, B). The 2-cyclic analogs appeared to be more effective in 6 mM than in 3 mM glucose, but the observed differences were not statistically significant. However, in 10 mM glucose, the 2-cyclic derivatives (10^{-9} M-10^{-7} M) were less effective (Fig. 4C).

Bell-shaped concentration-response curves were observed with the effective 2-cyclic-1,4-benzoxazine derivatives in the native pancreatic beta cells (Fig. 4A). All of the effective 2-cyclic-

JPET Fast Forward. Published on October 25, 2011 as DOI: 10.1124/jpet.111.185835
This article has not been copyedited and formatted. The final version may differ from this version.

1,4-benzoxazine derivatives showed a reduced efficacy at concentrations >10^{-9} M. The 2-phenyl analog (10^{-11}-10^{-6}M) was the most potent and effective compound in enhancing the KATP currents; its DE_{50} was 0.04±0.01x10^{-9}M (Fig 3A, Table 1). The 2-cyclohexylmethyl analog (10^{-10}-10^{-7}M) was less effective, while the 2-phenylethyl analog (10^{-10}-10^{-7}M) did not affect the KATP current (Fig. 4A, C).

The percentage activation of the currents by 2.5x10^{-4}M diazoxide were 220±12%, 400±20% and 150±11% (number of cells=6) with respect to the controls in 3 mM glucose and 5 mM NaN_3, 6 mM glucose and 10 mM glucose, respectively. A 2.5x10^{-4}M concentration of diazoxide in 3 mM glucose enhanced the whole cell currents from 43±5 pA in the control to 140±7 pA; and in 6 mM glucose from 27±6 pA and 137±9 pA in the control and following the application of the drug to the cells, respectively (Fig. 4A, B). A significant channel activation was observed also in 10 mM glucose (Fig 4C).

Partial inhibitory responses of the Kir6.2ΔC36 channel were observed with the 2-cyclic analogs (Table 1).

The application of the 2-*n*-hexyl-1,4-benzoxazine derivative in 3 mM glucose and 5 mM NaN_3 induced a dose-dependent cell depolarization that was recorded in the current-clamp mode (Fig. 5B). In 6 mM glucose, this compound also depolarized the cells, but the 2-isopropyl analog was inactive (Fig. 5A). The 2-phenyl analog hyperpolarized the cells at subnanomolar concentrations, but it did not cause a significant cell depolarization at higher concentrations (Fig. 5A, B). The 2-benzyl analog showed about 20 mV cell hyperpolarization at subnanomolar concentrations (Fig. 5A). The 2-*n*-hexyl analog induced insulin release in vitro, while the 2-phenyl analog reduced this insulin release (Fig. 6).

In the excised patch experiments, 10^{-6}M of the 2-*n*-hexyl analog caused a channel block of 64±5% (number of patches=3) in the presence of ATP and 59±4% (number of patches=3) in the

JPET Fast Forward. Published on October 25, 2011 as DOI: 10.1124/jpet.111.185835
This article has not been copyedited and formatted. The final version may differ from this version.

absence of the nucleotide. This blocking action was reversed following a 4 sec washout. The mean currents were -30±1 pA in the control, -13.2±0.4 pA in the presence of the 2-*n*-hexyl analog (10^{-6} M) and 10^{-4}M ATP, -12.1±1 pA in the presence of the 2-*n*-hexyl analog alone (10^{-6} M), -28±0.9 pA following the washout of the drug solution, and -4.5±0.3 pA with 10^{-4}M ATP (Fig. 7A). No effects were observed on the single channel conductance, which was 68±2 pS and 67±3 pS (number of patches=3) in the control and in the presence of a 10^{-6}M concentration of the drug, respectively. A 10^{-9}M concentration of the 2-phenyl analog led to a channel activation of 59±4% (number of patches=3) in the presence of 10^{-4} M internal ATP, but it produced a reduction of channel activity at a 10^{-7}M concentration. The mean currents were -31.5±1 pA in the control, -20.3±0.4 pA in the presence of the 2-phenyl analog (10^{-9} M) and 10^{-4}M ATP, -7.1±0.3 pA with the 2-phenyl analog (10^{-7} M) and 10^{-4}M ATP, -24.4±3 pA following the washout of the drug solution, and -4.3±0.4 pA with 10^{-4}M ATP (Fig. 7B).

In the presence of $2x10^{-4}$ M ADP, 10^{-9}M of the 2-phenyl analog led to a channel activation of 81±6% (number of patches=3) with respect to control, while a mild reduction of channel activity was observed at a 10^{-7} M concentration (number of patches=3) (Fig. 7C). The mean currents were -29.1±1 pA in the control, -36.2±2 pA with $2x10^{-4}$M ADP, -51±4 pA with the 2-phenyl analog (10^{-9}M) and $2x10^{-4}$M ADP, -23±1 pA with the 2-phenyl analog (10^{-7} M) and $2x10^{-4}$M ADP, -25.1±2 pA following the washout of the drug solution, and -3.5±0.3 pA with 10^{-4}M ATP (Fig. 7C). The 2-isopropyl analog failed to affect the KATP channel in the excised-patch experiments (data not shown).

In vivo effects of the 2H-1,4-benzoxazine derivatives on the AUC curves and fasting glucose levels in normal mice. No macroscopic signs of intolerability were observed in the benzoxazine derivative-treated mice. The mice did not show any type of local reaction following

the acute i.p. administration of a single dose of these compounds. No adverse effects were observed at 24 hrs or 14 days post-dose or thereafter.

The in vivo effects of the 2-isopropyl, 2-*n*-hexyl and 2-phenyl analogs were evaluated by IGTT and compared with the effects of glibenclamide or diazoxide. In the control mice that were injected with the vehicle, the administration of 2 g kg^{-1} of glucose 30 min before the first blood glucose measurement resulted in a typical increase in blood glucose levels from a basal value of 0.86±0.1 mg ml^{-1} to a peak of 2.72±0.7 mg ml^{-1} as shown in Fig. 8A. The administration of the 2-*n*-hexyl analog led to a bimodal response on glucose disposal; at a 0.2 mg kg^{-1} dose, the blood glucose levels changed from a basal value of 0.6±0.07 mg ml^{-1} to a peak of 3.31±0.9 mg ml^{-1}. However, the group injected with 10 mg kg^{-1} of the 2-*n*-hexyl analog showed an improvement in the glucose tolerance curve; their blood glucose levels increased from a basal value of 0.66±0.06 mg ml^{-1} to a peak of 1.64±0.8 mg ml^{-1}. No significant differences were observed in the peak glucose levels of the mice that were treated with the 2-isopropyl analog with respect to the vehicle-treated mice. The administration of 10 mg kg^{-1} of a 2-phenyl analog caused an increase of the glucose level from a basal value of 0.67±0.06 mg ml^{-1} to a peak of 3.3±0.9 mg ml^{-1}. A dose of 25 mg kg^{-1} diazoxide caused an enhancement of the glucose levels from a basal value of 0.68±0.08 mg ml^{-1} to a peak of 4.14±0.4 mg ml^{-1} (Fig. 8A). The animals that were treated with 2 mg kg^{-1} glibenclamide showed the most significant improvement in the glucose tolerance curve, with a peak glucose of 0.89±0.07 mg ml^{-1} (Fig. 8A).

The administration of increasing doses (0.2, 2 and 10 mg kg^{-1}) of the 2-*n*-hexyl analog led to a bimodal response in the AUC of blood glucose. In fact, at the lower dose of 0.2 mg kg^{-1}, the compound significantly increased the AUC values with respect to the vehicle; however, at a higher dose of 10 mg kg^{-1}, the 2-*n*-hexyl analog significantly decreased the AUC (Table 2). The 2-isopropyl analog increased the AUC values at the higher dose. The glibenclamide treatment (0.2

JPET Fast Forward. Published on October 25, 2011 as DOI: 10.1124/jpet.111.185835
This article has not been copyedited and formatted. The final version may differ from this version.

and 2 mg kg^{-1}) significantly decreased the AUC values with respect to the vehicle treated-group. The 2-phenyl analog (2-30 mg kg^{-1}) increased the AUC in a dose-dependent manner, and diazoxide (25 mg kg^{-1}) caused the maximal observed AUC increase (Table 2).

The 2-*n*-hexyl, 2-isopropyl and 2-phenyl analogs did not significantly affect the fasting blood glucose levels of the mice when compared to the 2 mg kg^{-1} dose of glibenclamide (Fig. 8B).

Discussion

In the present work, we showed that the 2-*n*-hexyl-1,4-benzoxazine derivative is a reversible, potent blocker of the KATP channels of native pancreatic beta cells, which leads to cell depolarization at nanomolar concentrations. Other Kir6.2 blockers that showed glucose-lowering effects exerted their action at micromolar concentrations, and they include the polyamine analogs; the vasodilating iptakalim; the synthetic imidazolines; the antipsychotics haloperidol and olanzepine; the antiarrhythmics cibenzoline, disopyramide and mexiletine; the antimalarials mefloquine and quinine; and the antibiotics lomefloxacin and gatifloxacin (Loussouarn et al., 2005; Bleck et al., 2005; Zünkler, 2006; Misaki et al., 2007). The 2-*n*-hexyl analog equally blocked the KATP channels of the native beta cells in the perforated and conventional whole-cell patch clamp methodologies and in the cells that expressed the truncated Kir6.2 subunit in the absence of SURs; these results suggest that the Kir6.2 subunit carries the inhibitory site(s) for this molecule.

The 2-*n*-hexyl analog showed anti-hyperglycemic activity in the IGT test, but it was less effective than glibenclamide. A biphasic behavior was observed in the glucose disposal curves that were determined in vivo following the administration of increasing doses of the 2-*n*-hexyl analog; these data can be explained by accounting for the opposite in vitro effects of this compound on pancreatic beta cells and skeletal muscle KATP channels (Fig. 9) (Tricarico et al., 2008).

JPET Fast Forward. Published on October 25, 2011 as DOI: 10.1124/jpet.111.185835
This article has not been copyedited and formatted. The final version may differ from this version.

The 2-phenyl analog activated the pancreatic KATP-channels at subnanomolar concentrations in the perforated patch-clamp mode; the activation of these channels induces cell hyperpolarization. This activation was more potent but less effective than diazoxide. The rank order of potency and efficacy of the channel openers was 2-phenyl>2-benzyl>2-cyclohexylmethyl analogs, while the 2-phenylethyl analog was not effective. Other pancreatic KATP-channel openers that activate the channel at nanomolar concentrations include the thiadiazine-dioxide analogs, such as the NN414, 7-chloro-3-isopropylamino-4*H*-1,2,4-benzothiadiazine-1,1-dioxide (BPDZ-73), 6-chloro-3-(1-methyl-1-phenylethyl)amino-4*H*-thieno[3,2-*e*]-1,2,4-thiadiazine-1,1-dioxide, NNC55-0462, and 6-chloro-3-cyclobutylamino-4*H*-1,2,4-benzothiadiazine-1,1-dioxide (Nielsen et al., 2006; Carosati, et al., 2007; Judge and Smith, 2009; Fischer et al., 2010; Pirotte et al., 2010).

The actions of the 2-cyclic aromatic analogs were mostly observed in the presence of medium and low glucose concentrations, while they were less effective in the presence of high external glucose, which suggests that they require a proper ATP/ADP ratio. This hypothesis is confirmed by the fact that in excised patch experiments, the 2-phenyl analog is capable of activating the KATP channel in the presence of ATP and ADP. However, the 2-cyclic analogs showed a reduced efficacy in activating the KATP channel currents at a concentration $>10^{-9}$ M; this concentration can be related to the low affinity interaction of these molecules with the Kir6.2 subunit. This is supported by the fact that these molecules inhibited the truncated Kir6.2 subunit in the nanomolar concentration range, but they showed a lower efficacy than the 2-linear alkyl chain analog.

As expected for a KATP channel opener, the 2-phenyl analog is the most effective 2*H*-1,4-benzoxazine derivative in increasing the AUC curve in normal mice, and this effect is similar to that of diazoxide; however, diazoxide caused the maximal observed increase of the AUC.

The introduction of a branched alkyl chain at position 2 of the 2*H*-1,4-benzoxazione nucleus leads to the formation of an inactive compound on the pancreatic KATP channel, as in the case of

the 2-isopropyl analog; however, this analog is effective on the skeletal muscle subtype (Tricarico et al., 2008).

The 2-isopropyl analog induced a dose-dependent enhancement of the AUC of the blood glucose; this result can be related to the activating action of the skeletal muscle KATP channels (Fig. 9).

Although glibenclamide affected the fasting blood glucose levels of the normal mice, the 2-*n*-hexyl, 2-phenyl and 2-isopropyl-1,4-benzoxazine derivatives did not affect the fasting blood glucose levels of these mice. These compounds did not affect the fasting glucose levels in respect to the glibenclamide because of their different modes of action on the target tissues. For example, the decrease of blood glucose due to the insulinotropic effect of the 2-*n*-hexyl analog is somehow counterbalanced by the KCO action on the skeletal muscle subtype. The actions of these drugs on neuronal KATP channels should be also considered. This specific channel controls the electrical activity of many types of neurons that are sensitive to the glucose level thereby influencing glucose homeostasis. For example, a reduction in extracellular glucose causes the opening of the KATP channels in glucose-sensitive neurons of the ventromedial hypothalamus, which triggers adrenaline-dependent glucagon secretion and the counter-regulatory response to hypoglycemia. The KATP channel activation, which is sufficient to abolish the electrical activity of the pro-opiomelanocortin (POMC)-expressing neurons in the arcuate nucleus, leads to hyperphagia and an increased body weight. Their partial activation, which reduces but does not abolish electrical activity, prevents glucose sensing and leads to an impaired glucose tolerance (McTaggart et al., 2010).

The differences in the kinetics of the actions of these compounds, which are rapidly reversible with the linear alkyl chain derivative as compared with the sulfonylurea compound, may also play a role.

In conclusion, the 2-linear alkyl chain is the molecular determinant that confers the blocking action to the 2*H*-1,4-benzoxazines in pancreatic beta cells, while the branched substituent is the molecular determinant that confers the activating action in skeletal muscles. The aromatic substituent confers the opening action to the 2*H*-1,4-benzoxazines in both the pancreatic beta cells and the skeletal muscle cells. SUR1 shows an overall identity of 79% with SUR2A; larger differences exist in the amino acid sequences of the first nucleotide binding fold-2 (NBF2) and second transmembrane domain (TMD2) regions, and additional minor differences were found in the NBF2 region (Moreau et al., 2005). The NBF2 region confers sensitivity to the SUR2 openers with a benzopyran-like structure (cromakalim) and the pyridine (pinacidil) (Moreau et al., 2005). We propose that the 2-isopropyl 1,4-benzoxazine, which is a structurally related analog of nucleotides, can bind to a site that is located on the NBF2 of SUR2A, although its interaction with the TMD2 cannot be excluded. The 2-*n*-hexyl analog blocks the pancreatic and skeletal muscle KATP channels by interacting with the Kir6.2 subunit, but it also activates the muscle KATP channel by potentially interacting with the TMD2-NBF2 region. The 2-phenyl 1,4-benzoxazine activates both the pancreatic beta cells and the skeletal muscle channels with a comparable potency and efficacy. These actions can be mediated by the binding of a drug to the TMD2-NBF2 region and to an additional site located on TMD1-NBF1, which is the main region that is responsible for the binding and activation of the pancreatic beta cell KATP channel by diazoxide (Babenko et al., 2000; Moreau et al., 2005) (Fig. 9).

The 2-*n*-hexyl analog action that is mediated by the Kir6.2 subunit is an alternative mechanism of action with respect to that of the hypoglycemic sulfonylureas that target SUR1. This can be related to the structural similarity of this compound with the ATP molecule (Tricarico et al., 2008). The 2-phenyl analog may represent a potential drug treatment in patients who are intolerant to diazoxide. The 2*H*-1,4-benzoxazines have a differential pharmacological profile with respect to the SUR1 blockers or openers; in vitro and in vivo, they show a combined activating/blocking

action toward KATP channels that confers a significant glycemic control following the administration of a glucose bolus, but they do not affect fasting glycemia. Additionally, their opening action of the skeletal muscle KATP channels may be cytoprotective, although pure SUR2A openers may lead to arrhythmia (Jahangir and Terzic, 2005). A similar mechanism has been proposed for iptakalim, which is a potent sub-nanomolar vascular KATP channel opener. At a high micromolar concentration, iptakalim shows a blocking action of the pancreatic channel, and it is in clinical development as an antihypertensive drug (Misaki, et al., 2007; Pan et al., 2010).

Acknowledgments. Manuscript editing was performed with the contribution of the American Journal Experts (AJE).

Authorship contributions.

Participated in research design: Tricarico, and Rolland.

Conducted experiments: Rolland, Cannone, Cippone, and Mele.

Contributed new reagents or analytic tools: Carbonara, Loiodice, Laghezza, Fracchiolla, and Tortorella.

Performed data analysis: Mele, and Cannone.

Wrote or contributed to the writing of the manuscript: Tricarico, Mele, and Conte Camerino.

References

Arnoux JB, de Lonlay P, Ribeiro MJ, Hussain K, Blankenstein O, Mohnike K, Valayannopoulos V, Robert JJ, Rahier J, Sempoux C, Bellanné C, Verkarre V, Aigrain Y, Jaubert F, Brunelle F, and Nihoul-Fékété C (2010) Congenital hyperinsulinism. *Early Hum Dev* **86(5)**: 287-94. Epub 2010 Jun 13. Review.

Ashcroft FM **(**2010) New uses for old drugs: neonatal diabetes and sulphonylureas. Cell *Metabolism* **11**: 179-181.

Babenko AP, Gonzalez G, and Bryan J (2000) Pharmaco-topology of Sulfonylurea Receptors SEPARATE DOMAINS OF THE REGULATORY SUBUNITS OF *K*ATP CHANNEL ISOFORMS ARE REQUIRED FOR SELECTIVE INTERACTION WITH K^+ CHANNEL OPENERS. *The J Biol Chem* **275/2** : 717–720.

Bleck C, Wienbergen A, and Rustenbeck I (2005) Essential role of the imidazoline moiety in the insulinotropic effect but not the KATP channel-blocking effect of imidazolines; a comparison of the effects of efaroxan and its imidazole analog, KU14R. *Diabetologia* **48:** 2567–2575.

Carosati E, Mannhold R, Wahl P, Hansen JB, Fremming T, Zamora I, Cianchetta G, and Baroni M (2007) Virtual screening for novel openers of pancreatic K(ATP) channels. *J Med Chem* **50:** 2117-2126.

Fischer A, Schmidt C, Lachenicht S, Grittner D, Winkler M, Wrobel T, Rood A, Lemoine H, Frank W, and Braun M (2010) Synthesis of Benzofuran, Benzothiophene, and Benzothiazole-Based Thioamides and their Evaluation as KATP Channel Openers. *Chem Med Chem* **5:** 1749 – 1759.

Flanagan SE, Patch AM, Mackay DJ, Edghill EL, Gloyn AL, Robinson D, Shield JP, Temple K, Ellard S, Hattersley AT **(**2007) Mutations in ATP-sensitive K^+ channel genes cause transient neonatal diabetes and permanent diabetes in childhood or adulthood. *Diabetes* **56**:1930-1937.

Flechtner I, de Lonlay P, and Polak M (2006) Diabetes and hypoglycaemia in young children and mutations in the Kir6.2 subunit of the potassium channel: therapeutic consequences. *Diabetes Metab* **6**:569-580.

Gribble FM and Reimann F (2003) Sulphonylurea action revisited: the post-cloning era. *Diabetologia* **46:**875–891.

Hambrock A, de Oliveira Franz CB, Hiller S, and Osswald H (2006) Glibenclamide-induced apoptosis is specifically enhanced by expression of the sulfonylurea receptor isoform SUR1 but not by expression of SUR2B or the mutant SUR1(M1289T). *J Pharmacol Exp Ther* **316(3):**1031-1037.

Hansen JB (2006) Towards selective Kir6.2/SUR1 potassium channel openers, medicinal chemistry and therapeutic perspectives. *Curr Med Chem* **13(4)**: 361-376.

Hussain K (2007). Insights in congenital hyperinsulinism. *Endocr Dev* **11:**106-121.

Jahangir A and Terzic A (2005) KATP channel therapeutics at the bedside. *J Mol Cell Cardiol* **39**: 99–112.

Judge S IV and Smith PJ (2009) Patents related to therapeutic activation of KATP and K2P potassium channels for neuroprotection: ischemic/hypoxic/anoxic injury and general anesthetics *Expert Opin Ther Patents* **19(4):** 433-460.

Juhl K and Hutton J (2004) Stimulus–secretion coupling in the pancreatic beta-cell. *Adv Exp Med Biol* **552**: 66–90.

Koster J C, Permutt MA, and Nichols CG (2005) Diabetes and insulin secretion: the ATP-sensitive K^+ channel (KATP) connection. *Diabetes* **54:**3065-3072.

Loussouarn G, Marton L J, and Nichols CG (2005) Molecular Basis of Inward Rectification: Structural Features of the Blocker Defined by Extended Polyamine Analogs. *Mol Pharmacol* **68:** 298–304.

Maedler K, Carr RD, Bosco D, Zuellig RA, Berney T, and Donath MY (2005) Sulfonylurea induced beta-cell apoptosis in cultured human islets. *J Clin Endocrinol Metab* **90:**501-506.

McTaggart J S, Clark R H, and Ashcroft F M (2010) The role of the KATP channel in glucose homeostasis in health and disease: more than meets the islet. *J Physiol* **588.17** : 3201–3209.

Misaki N, Mao X, Lin Y, Suga S, Li G, Liu Q, Chang Y, Wang H, Wakui M, and Wu J (2007) Iptakalim, a Vascular ATP-Sensitive Potassium (KATP) Channel Opener, Closes Rat Pancreatic beta-Cell KATP Channels and Increases Insulin Release. *JPET* **322**: 871–878.

Mlynarski W, Tarasov AI, Gach A, Girard CA, Pietrzak I, Zubcevic L, Kusmierek J, Klupa T, Malecki MT, Ashcroft FM (2007) Sulfonylurea improves CNS function in a case of intermediate DEND sindrome caused by a mutation in KCNJ11. *Nat Clin Pract Neurol* **11**:640-645.

Moreau C, Prost A, Dérand R, and Vivaudou M (2005) SUR, ABC proteins targeted by KATP channel openers. *J Mol Cell Cardiol* **38**: 951–963.

Nielsen FE, Ebdrup S, Jensen AF, Ynddal L, Bodvarsdottir TB, Stidsen C, Worsaae A, Boonen HCM, Arkhammar POG, Fremming T, Wahl P, Kornø HT, and Hansen JB (2006) New 3-Alkylamino-4H-thieno-1,2,4-thiadiazine 1,1-Dioxide Derivatives Activate ATP-Sensitive Potassium Channels of Pancreatic Beta Cells. *J Med Chem* **49:** 4127-4139.

Nourparvar A, Bulotta A, Di Mario U, and Perfetti R (2004) Novel strategies for the pharmacological management of type 2 diabetes. *Trends Pharmacol Sci* **25**:86-91.

Pan Z, Huang J, Cui W, Long C, Zhang Y, and Wang H (2010) Targeting Hypertension with a New Adenosine Triphosphate Sensitive Potassium Channel Opener Iptakalim. *Cardiovascular Pharmacol* **56**: 215-228.

Pearson ER, Flechtner I, Njølstad PR, Malecki MT, Flanagan SE, Larkin B, Ashcroft FM , Klimes I, Codner E, Iotova V, Slingerland AS, Shield J, Robert J-J, Holst JJ, Clark PM, Ellard S, Søvik O, Polak M, and Hattersley AT (2006) Switching from insulin to oral sulfonylureas in patients with diabetes due to Kir6.2 mutations. *N Engl J Med* **355:**467-477.

Pirotte B, De Tullio P, Nguyen Q, Somers F, Fraikin P, Florence X, Wahl P, Hansen JB, and Lebrun P (2010) Chloro-Substituted 3-Alkylamino-4H-1,2,4-benzothiadiazine 1,1-Dioxides as ATP-Sensitive Potassium Channel Activators: Impact of the Position of the Chlorine Atom on the Aromatic Ring on Activity and Tissue Selectivity. *J Med Chem* **53**: 147–154.

Rolland JF, Henquin JC, Gilon P (2002) Feedback control of the ATP-sensitive K^+ current by cytosolic Ca^{2+} contributes to oscillations of the membrane potential in pancreatic beta-cells. *Diabetes* **51**: 376–384.

Rolland JF, Tricarico D, Laghezza A, Loiodice F, Tortorella V, and Camerino DC (2006) A new benzoxazine compound blocks KATP channels in pancreatic beta cells: molecular basis for tissue selectivity in vitro and hypoglycaemic action in vivo. *Br J Pharmacol* **149:** 870-879.

Seino S and Mikia T (2003) Physiological and pathophysiological roles of ATP-sensitive K^+ channels. Progress. *Biophysics & Molecular Biology* **81**: 133–176.

Simard M J, Woo SK, Bhatta S, and Gerzanich V (2008) Drugs acting on SUR1 to treat CNS ischemia and trauma. *Curr Opin Pharmacol* **8**: 42–49.

Takahashi A, Nagashima K, Hamasaki A, Kuwamura N, Kawasaki Y, Ikeda H, Yamada Y, Inagaki N, and Seino Y (2007) Sulfonylurea and glinide reduce insulin content, functional expression of K(ATP) channels, and accelerate apoptotic beta-cell death in the chronic phase. *Diabetes Res Clin Pract* **77**: 343-350.

Teshima Y, Akao M, Li RA, Chong TH, Baumgartner WA, Johnston MV, and Marbán E (2003) Mitochondrial ATP-sensitive potassium channel activation protects cerebellar granule neurons from apoptosis induced by oxidative stress. *Stroke* **34:** 1796-1802.

Tricarico D, Barbieri M, Antonio L, Tortorella P, Loiodice F, and Camerino DC (2003) Dualistic actions of cromakalim and new potent 2H-1,4-benzoxazine derivatives on the native skeletal muscle KATP channel. *Br J Pharmacol* **139:** 255-262.

Tricarico D, Mele A, Camerino GM, Bottinelli R, Brocca L, Frigeri A, Svelto M, George A L Jr, and Conte Camerino D (2010) The KATP channel is a molecular sensor of atrophy in skeletal muscle. *J Physiol* **588:** 773–784.

Tricarico D, Mele A, Camerino GM, Laghezza A, Carbonara G, Fracchiolla G, Tortorella P, Loiodice F, and Camerino DC (2008) Molecular determinants for the activating/blocking actions of the 2H-1,4-benzoxazine derivatives, a class of potassium channel modulators targeting the skeletal muscle KATP channels. *Mol Pharmacol* **74:** 50-58.

Zünkler B J (2006) Human ether-a-go-go-related (HERG) gene and ATP-sensitive potassium channels as targets for adverse drug effects. *Pharmacol & Ther* **112:** 12–37.

Footnotes. This work was supported by the Italian Telethon [Grant GGP10101].

[1] The authors Domenico Tricarico[1] and Jean-François Rolland [1] equally contributed to the work.

Legends for figures

Fig. 1. Chemical structure of the newly synthesized 2-*H*-1,4-benzoxazine derivatives that were tested on the pancreatic KATP channels.

Fig. 2. Protocols used for the identification of the pancreatic beta cells and islets. Sample traces of KATP currents were recorded using a perforated patch-clamp in the whole-cell mode from beta cells that were first exposed to a bath solution that was enriched with 10 mM glucose followed by 3 mM glucose+5 mM NaN_3 or 6 mM glucose solutions (A). The currents were recorded during pulses of ±20 mV (Vm) from a holding potential of –70 mV (Vm) (O indicates the open channel levels as upward or downward deflections of the current record, and C indicates the closed level). The decrease in the external glucose concentration led to the enhancement of the whole-cell currents. The responses of the current following the application of diazoxide (Diazo.) or tolbutamide (Tolb.) in the presence of 3 mM glucose+5 mM NaN_3, and a washout of the drug solution are represented. Diazoxide increased the whole-cell current, while tolbutamide reduced it, and their effects were reversible. Sample traces of the membrane potentials versus time from the beta cells that were exposed to different concentrations of glucose were recorded in the current clamp mode (B). The exposure of the beta cells to increasing external glucose led to cell depolarization and firing. The insulin secretion was induced by low or high levels of external glucose and the residual insulin content in the islets (C). Batches of 8 islets were incubated with different concentrations of external glucose for insulin release; the insulin content of the islets was evaluated following ethanol and HCl extraction. Each bar is the mean ±E.S. of three values.

JPET Fast Forward. Published on October 25, 2011 as DOI: 10.1124/jpet.111.185835
This article has not been copyedited and formatted. The final version may differ from this version.

Fig. 3. Effects of the 2-isopropyl- and 2-*n*-hexyl-1,4-benzoxazine derivatives on the KATP currents of the mouse pancreatic beta cells and on the Kir6.2ΔC36 channel that was expressed in the HEK293 cells. Sample traces of the whole-cell KATP currents were recorded in the pancreatic beta cells during pulses of ±20 mV (Vm) from a holding potential of –70 mV (Vm); the measurements were performed in the absence (control, Ctrl) or presence of drugs and with different external glucose concentrations using the perforated patch mode or the conventional whole-cell mode. The Kir6.2ΔC36 current was recorded in the HEK293 cells using the conventional whole-cell patch during a pulse of -100 mV (Vm). O indicates the open channel levels as upward or downward deflections of the current record, and C indicates the closed level. Increasing concentrations of the same drug are indicated on the corresponding current traces. At -50 mV (Vm) using the perforated patch mode in 3 mM glucose+5 mM NaN_3 (A) and the conventional whole cell patch mode (B), the 2-*n*-hexyl analog, which showed a threshold concentration of 10^{-10} M in both experimental conditions, inhibited the KATP current with similar efficacy. The co-application of glibenclamide and the 2-*n*-hexyl analog to the beta cells enhanced the channel block induced by the 2-hexyl analog (B). The 2-*n*-hexyl analog reduced the Kir6.2ΔC36 current, and $BaCl_2$ caused a further reduction in the channel currents (C). In 6 mM glucose, the 2-*n*-hexyl analog inhibited the KATP current of the beta cell, which showed a threshold concentration $>10^{-10}$ M(D). Tolbutamide (Tolb.) almost fully reduced the currents (A, D). The average beta-cell KATP current density versus the 2*H*-1,4-benzoxazine or tolbutamide concentrations (10^{-8}-10^{-6}M) in 10 mM glucose. Each bar represents the mean±S.E. of the current data from 3 cells (E). The concentration-response relationships of the KATP currents of the beta cells versus the 2-isopropyl (black circles) and 2-*n*-hexyl-1,4-benzoxazine (black squares) concentrations that were constructed at -50 mV (Vm) in 3 mM glucose using the perforated patch or the whole-cell patch mode for 2-*n*-hexyl analog (white squares) (F). The concentration-response relationship of the Kir6.2ΔC36 currents versus the 2-*n*-hexyl analog

JPET Fast Forward. Published on October 25, 2011 as DOI: 10.1124/jpet.111.185835
This article has not been copyedited and formatted. The final version may differ from this version.

concentration (white triangle) constructed at -100 mV (Vm) using the conventional whole-cell patch mode (F). Each experimental point represents the mean±S.E. of the percentage inhibition of the KATP currents versus the drug concentrations of 3 cells; no more than 2 drug concentrations per cell were tested. * These data were significantly different from the controls for $p<0.05$.

Fig. 4. Effects of the 2-phenyl, 2-benzyl, 2-phenylethyl and 2-cyclohexyl methyl 1,4-benzoxazine derivatives on the KATP currents of the pancreatic beta cells in the presence 3 mM, 6 mM or 10 mM glucose. Sample traces of the whole-cell KATP currents were recorded using the perforated patch mode during pulses of ±20 mV (Vm) from a holding potential of –70 mV (Vm) in the absence (control, Ctrl) or presence of drugs and at different external glucose concentrations. O indicates the open channel levels as the upward or downward deflections of the current record, and C indicates the closed level. Different concentrations of the same drug are indicated on the corresponding current traces. The whole cell currents that were measured at -50 mV (Vm) in 3 mM glucose+5 mM NaN_3 were enhanced in respect to controls following the application of $0.7x10^{-10}$M and 10^{-10}M concentrations of the 2-phenyl analog and of a 10^{-10}M concentration of the 2-benzyl analog (A). A $2.5x10^{-4}$M concentration of diazoxide (Diazo.) in 3 mM glucose also increased the whole cell current (A). The concentration-response relationships of the KATP currents versus the 2-phenyl (black triangles), 2-benzyl (black rhomb), 2-phenylethyl (white triangles) and 2-cyclohexylmethyl (upside-down black triangles) analog concentrations constructed in 3 mM glucose and 5 mM NaN_3 in the bath at -50 mV (Vm) are shown. Each experimental point represents the mean ± S.E. of the percentage activation of the KATP currents versus the drug concentrations of 3 cells; no more than 2 drug concentrations per cell were tested (A). In 6 mM glucose, the whole currents were enhanced following the application of a 10^{-10} M concentration of the 2-phenyl and 2-benzyl analogs, and by $2.5x10^{-4}$M diazoxide (B). The average beta cell KATP current density versus the drug concentrations (10^{-9}-10^{-7}M) or diazoxide in 10 mM glucose are shown. Each bar represents the

JPET Fast Forward. Published on October 25, 2011 as DOI: 10.1124/jpet.111.185835
This article has not been copyedited and formatted. The final version may differ from this version.

mean±S.E. of the current data from 3 cells (C). *These data were significantly different from the controls for $p<0.05$.

Fig. 5. Effects of the 2*H*-1,4-benzoxazine derivatives on the membrane potential of the pancreatic beta cells in different external glucose concentrations. Time course of the membrane potentials of the pancreatic beta cells that were perfused with solutions containing 6 mM glucose in the absence or presence of 2-*n*-hexyl, 2-isopropyl, 2-phenyl or 2-benzyl-1,4-benzoxazine derivatives at 10^{-10}M or 10^{-7}M concentrations (A). Scatter plots of the membrane potentials in the absence (control, Ctrl) or presence of the drugs at different concentrations (10^{-9}-10^{-7}M) in 10 mM or 3 mM glucose and 5 mM NaN_3 (B). Each point represents the mean ± S.E. of the absolute values of the voltage data from three cells.

Fig. 6. Insulin secretion induced by low external glucose and residual insulin content in the islets. The drug effects on insulin release was evaluated in 3 mM glucose and 5 mM NaN_3 and compared with that obtained in the absence of the drugs (Contr.). Batches of 8 islets were incubated with the 2-*n*-hexyl (10^{-8}M), 2-isopropyl (10^{-7}M), 2-phenyl (10^{-9}M) and 2-benzyl (10^{-9}M) analogs. Each bar is the mean $\pm$E.S. of three values. *These data are significantly different from the controls for $p<0.05$.

Fig. 7. Effects of the 2-*n*-hexyl and 2-phenyl-1,4-benzoxazine derivatives on the channel currents that were recorded in the excised patches that contained multiple KATP channels from the pancreatic beta cells. The KATP channel currents were recorded in excised inside-out patches that were held at –50 mV (Vm) and in the presence of 140 mM KCl on both sides of the membrane. The drug solutions were applied to the internal sides of the patches with or without nucleotides using a

fast perfusion system. The 2-*n*-hexyl analog blocks channel currents in the presence and in the absence of internal ATP. Washout of drug solution rapidly restored channel currents (A). The 2-phenyl analog in the presence of the nucleotides increased the channel activity at low concentrations, but markedly inhibited it at the high concentration in the presence of internal ATP (B), and caused a mild inhibition of channel activity in the presence of internal ADP (C).

Fig. 8. Intraperitoneal glucose tolerance test and fasting glucose levels in the drug-treated mice. Sample curves representing the blood glucose levels of the mice that fasted for 14 hr and were then treated with the vehicle solution (a) or with vehicle solution that was enriched with either 0.2 mg kg^{-1} 2*n*-hexyl (b), 10 mg kg^{-1} 2-*n*-hexyl (c), 30 mg kg^{-1} 2-isopropyl (d), 10 mg kg^{-1} 2-phenyl (e), 25 mg kg^{-1} diazoxide (f) or 2 mg kg^{-1} glibenclamide (g) are shown. The mice were injected with the drug solutions or vehicle intraperitoneally (i.p.) at a constant volume of 0.15 ml 30 min before glucose loading. The mice were given 2 g kg^{-1} glucose via an i.p. injection immediately following the first glycemia determination (time 0). Blood was drawn from a tail vein at 0, 15, 30, 60 and 120 min, and the blood glucose level was measured by the glucose oxidase method (Glucometer Elite, Bayer-Schweiz-AG, Zurich, Switzerland) (A). The mean values of the initial (t=0) blood glucose level in the mice that fasted for 14 hr and were treated with the vehicle solution; a vehicle solution enriched with either 2-isopropyl, 2-*n*-hexyl or 2-phenyl-1,4-benzoxazine derivatives; or a vehicle solution enriched with glibenclamide (Glib.). The tail vein blood sample was taken 30 min after the treatment was administered (B). The data were significantly different for *$P<0.05$ with respect to the animal group that was treated with the vehicle.

Fig. 9. Hypothetical binding sites of the 2*H*-1,4-benzoxazine derivatives on the Kir6.2 subunit and SUR1 or SUR2. The 2-hexyl analog preferentially binds to the ATP sites of the Kir6.2 subunit and exerts its blocking action in the pancreatic beta cells and the skeletal muscles. This chemical showed an opening action in the skeletal muscle through its interaction with the nucleotide binding fold2 (NBF2) of SUR2A. The 2-isopropyl analog is a KATP channel agonist that interacts with the unique residues that are located in the NBF2 of SUR2A. The 2-phenyl analog activates both the pancreatic beta cells and the skeletal muscle KATP channels by possibly interacting with NBF2 of SUR2A and NBF1 of SUR1.

JPET Fast Forward. Published on October 25, 2011 as DOI: 10.1124/jpet.111.185835
This article has not been copyedited and formatted. The final version may differ from this version.

TABLE 1

Fitting parameters of the concentration response curves of the 2*H*-1,4 benzoxazine derivatives versus the pancreatic beta cell KATP channel currents, which were recorded using the perforated or conventional whole-cell patch clamp, and the Kir6.2ΔC36 channel currents that were expressed in HEK293 cells, which were recorded using the conventional whole-cell patch clamp.

	K ATP					Kir6.2ΔC36		
Compounds	I max (%)	Amax (%)	DE_{50} (10^{-9}M)	IC_{50} (10^{-9}M)	*n*	I max (%)	IC_{50} (10^{-9}M)	*n*
Linear								
2*n*-hexyl	-59.1±5	/	/	10.1±3	-0.5±0.1	-69.9±5*[(1)]	9.6±1*[(1)]	-0.7±0.1[(1)]
(10^{-10}-10^{-4}M)	N =10			N =10	N =10	N =4	N =4	N =4
	-68±5[(1)]			9.8±2 [(1)]	-1±0.1[(1)]			
	N =12			N=12	N =12			
Branched								
2-isopropyl	No effect	No	/	/	/	No effect[(1)]	/	/
(10^{-10}-10^{-4}M)	N =9	effect				N =6		
		N =9						
Cyclic								
2-phenyl	/	86.4±8*	0.04±0.01*	/	1.2±0.1	-31.1±2[(1)]	/	/
(10^{-11}-10^{-6}M)		N = 12	N = 12		N = 12	N =7		
2-benzyl	/	56.3±3*	0.06±0.01	/	1.3±0.1	/	>100[(1)]	/
(10^{-11}-10^{-6}M)		N =7	N =7		N =7		N =7	
2-phenylethyl	No effect	No	/	/	/	-30.2±4[(1)]	/	/
(10^{-10}-10^{-7}M)	N = 6	effect				N =4		
		N = 6						
2-cyclohexyl	/	19.3±4	/	/	/	-30±3[(1)]	>100[(1)]	/
methyl		N =6				N =6	N =6	
(10^{-10}-10^{-7}M)								

JPET Fast Forward. Published on October 25, 2011 as DOI: 10.1124/jpet.111.185835
This article has not been copyedited and formatted. The final version may differ from this version.

Table 1. These compounds are the 2*H*-1,4 benzoxazine derivatives that contain linear alkyl or cyclic groups at position 2 of the benzoxazine nucleus. The range of concentrations that was tested for each compound is given in parenthesis. The concentration-response curves for these drugs were constructed in the presence of 3 mM glucose in the bath in the pancreatic beta cells using the perforated (glucose+5 mM NaN_3) and/or conventional whole-cell recordings (1) and in the HEK293 cells that were transfected with the Kir6.2ΔC36 channel subunit using the conventional whole-cell recordings (1). Kir6.2ΔC36 is the truncated Kir6.2 subunit that was expressed in the cell line, while KATP is the native ATP-sensitive potassium channel of the pancreatic beta cell. * The data are significantly different from those of the other analogs in the same condition at $p<0.05$.

JPET Fast Forward. Published on October 25, 2011 as DOI: 10.1124/jpet.111.185835
This article has not been copyedited and formatted. The final version may differ from this version.

TABLE 2

Area under the curve (AUCs) data for the serum glucose concentration in the drug-treated mice.

Treatments	Dose ($mg \times kg^{-1}$)	AUC (mg x ml x min)	N° animals
Vehicle	/	217.38±12.41	5
Linear			
2*n*-hexyl	0.2	413.38±39.39*	4
	2	270.34±36.44	5
	10	150.64±23.04*	4
Branched			
2-isopropyl	2	197.85±45.22	3
	10	238.88±51.27	3
	30	259.58±38.82*	4
Cyclic			
2-phenyl	2	256.36±43.26	3
	10	339.03±27.62*	5
	30	393.03±31.31*	5
glibenclamide	0.2	128.08±15.44*	4
	2	103.23±25.41*	3
diazoxide	25	450.80±59.78*	3

Table 2. The area under the curves (AUCs) data were obtained during the i.p. glucose tolerance test in the fasted mice that were pretreated with the vehicle solution or the vehicle solution that was enriched with different doses of the 2*H*-1,4 benzoxazine derivatives. The AUCs were determined by using the fasting glucose concentration (t_0-value) as a reference to minimize the importance of the 'starting value'. The data were significantly different for *$P<0.05$ with respect with the animal group that was treated with the vehicle.

JPET Fast Forward. Published on October 25, 2011 as DOI: 10.1124/jpet.111.185835
This article has not been copyedited and formatted. The final version may differ from this version.

Figure 1

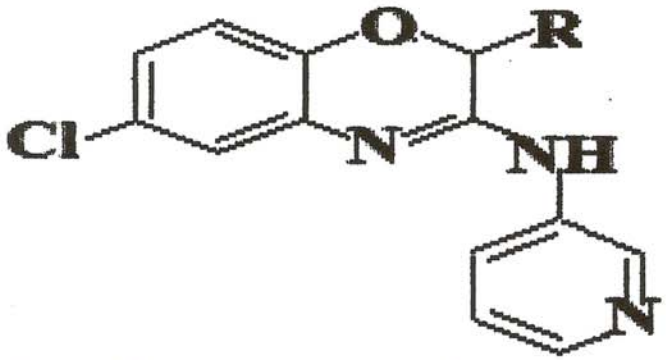

2H-1,4 benzoxazine nucleus

Compound	R
n-hexyl	
Isopropyl	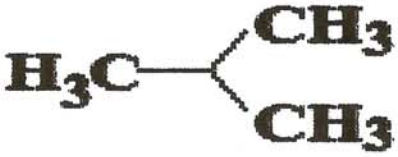
Phenyl	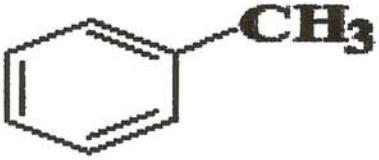
Benzyl	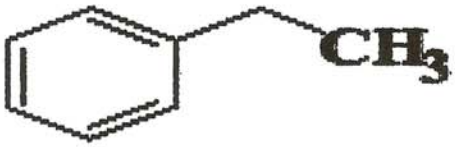
2-(phenyl)-ethyl	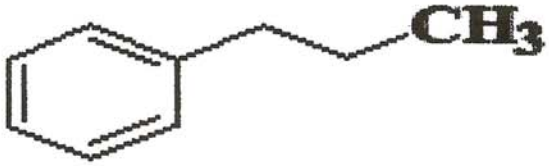
Cyclohexyl-methyl	

Figure 2

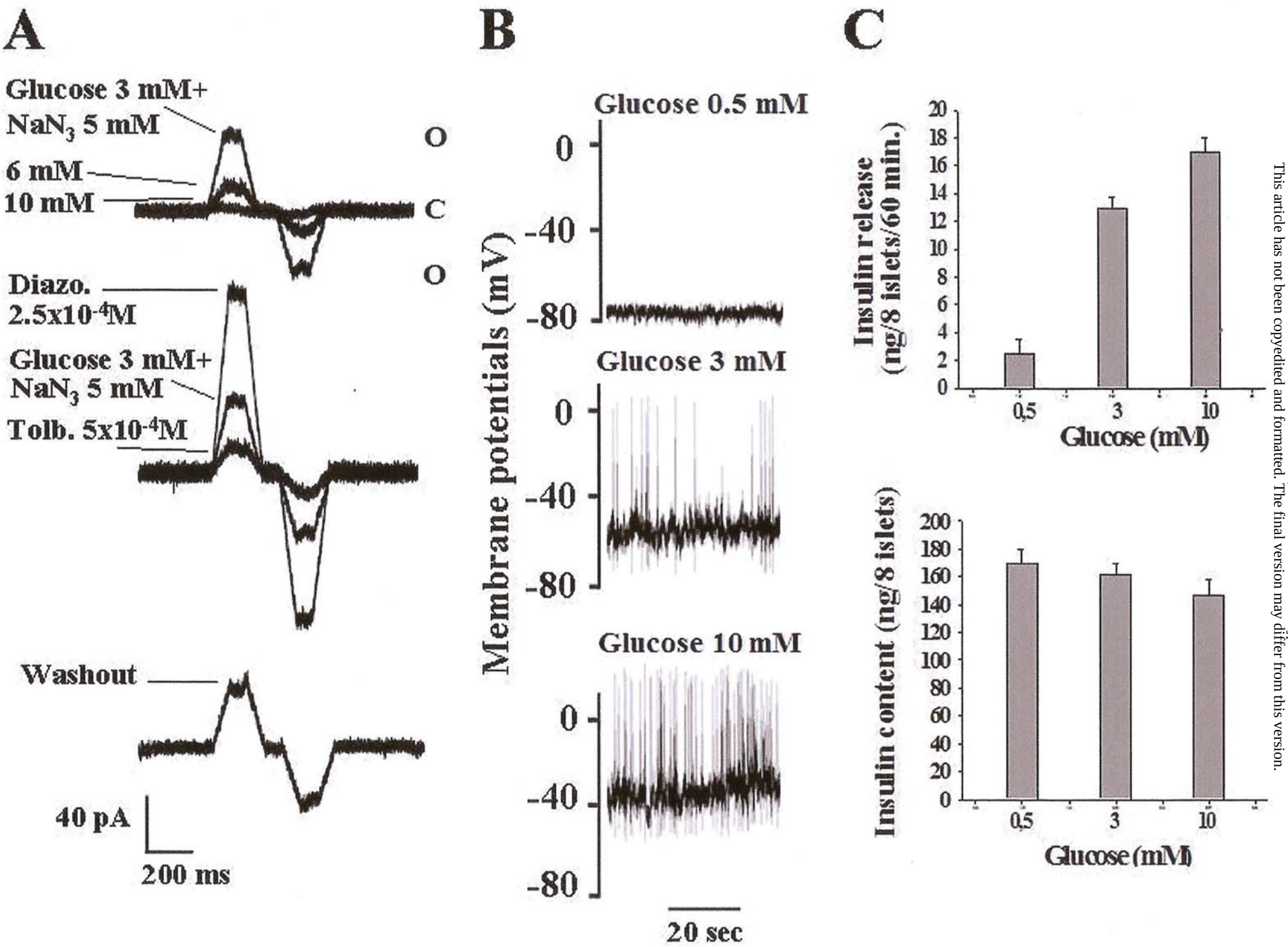

Figure 3

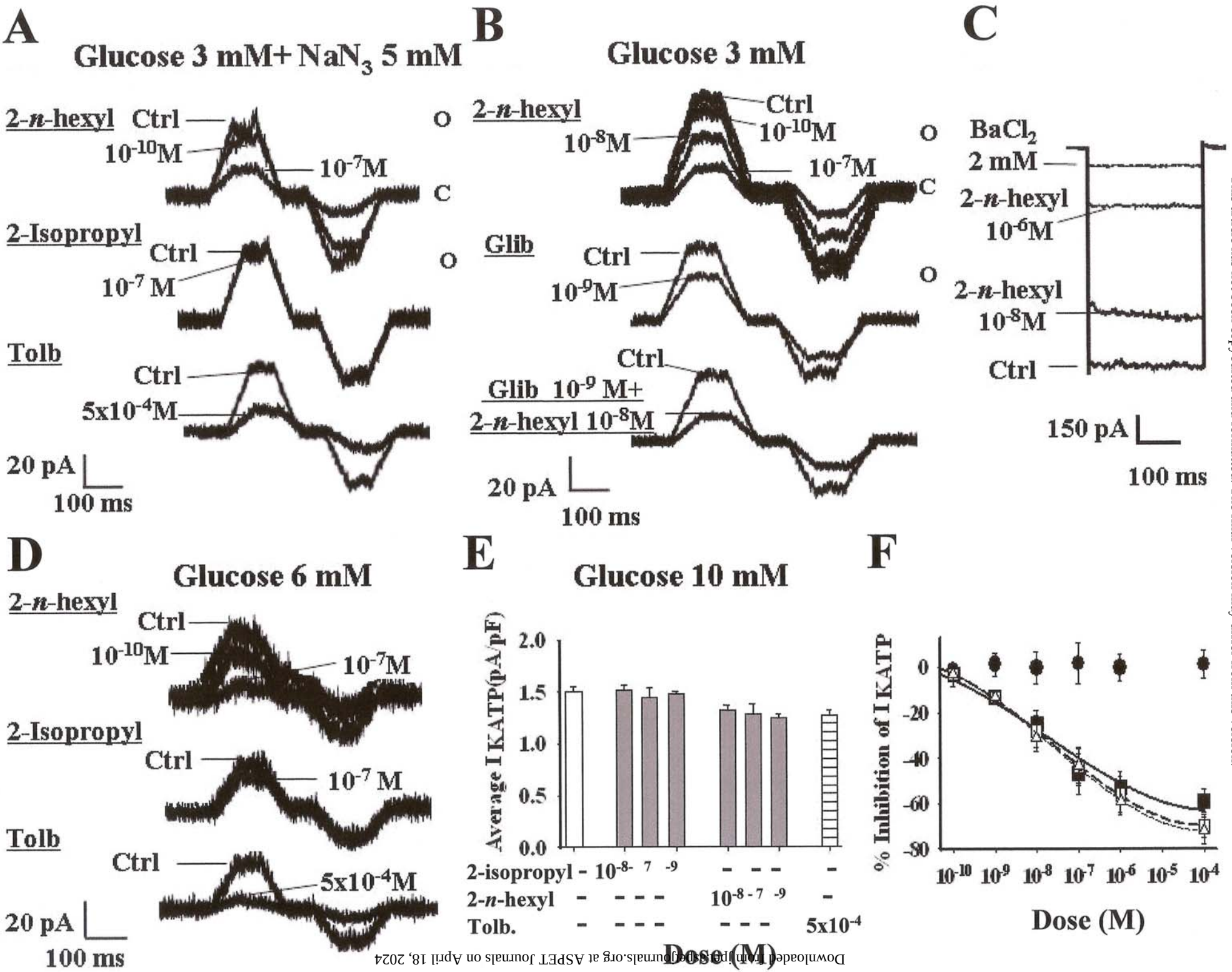

Figure 4

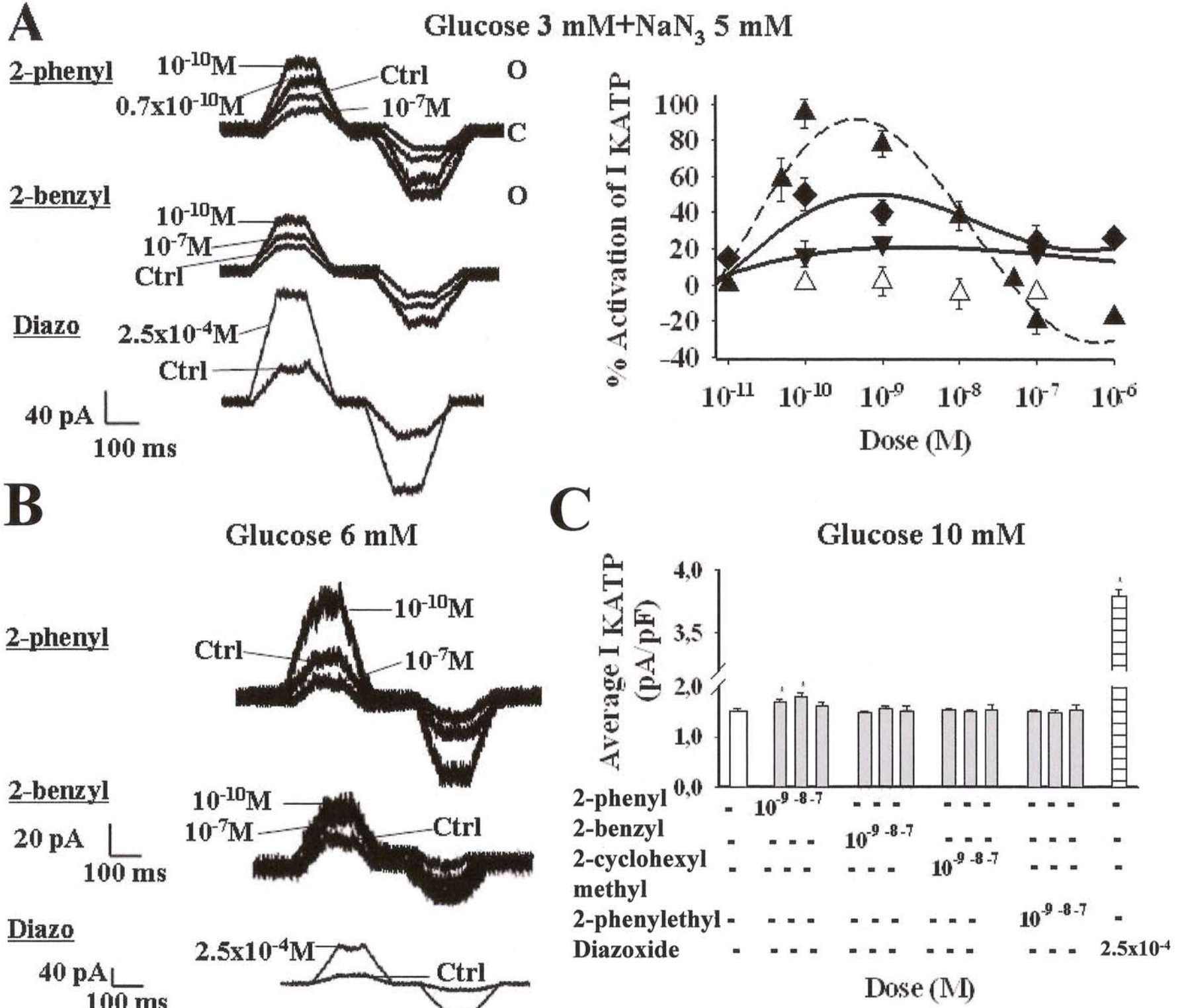

JPET Fast Forward. Published on October 25, 2011 as DOI: 10.1124/jpet.111.185835
This article has not been copyedited and formatted. The final version may differ from this version.

Figure 5

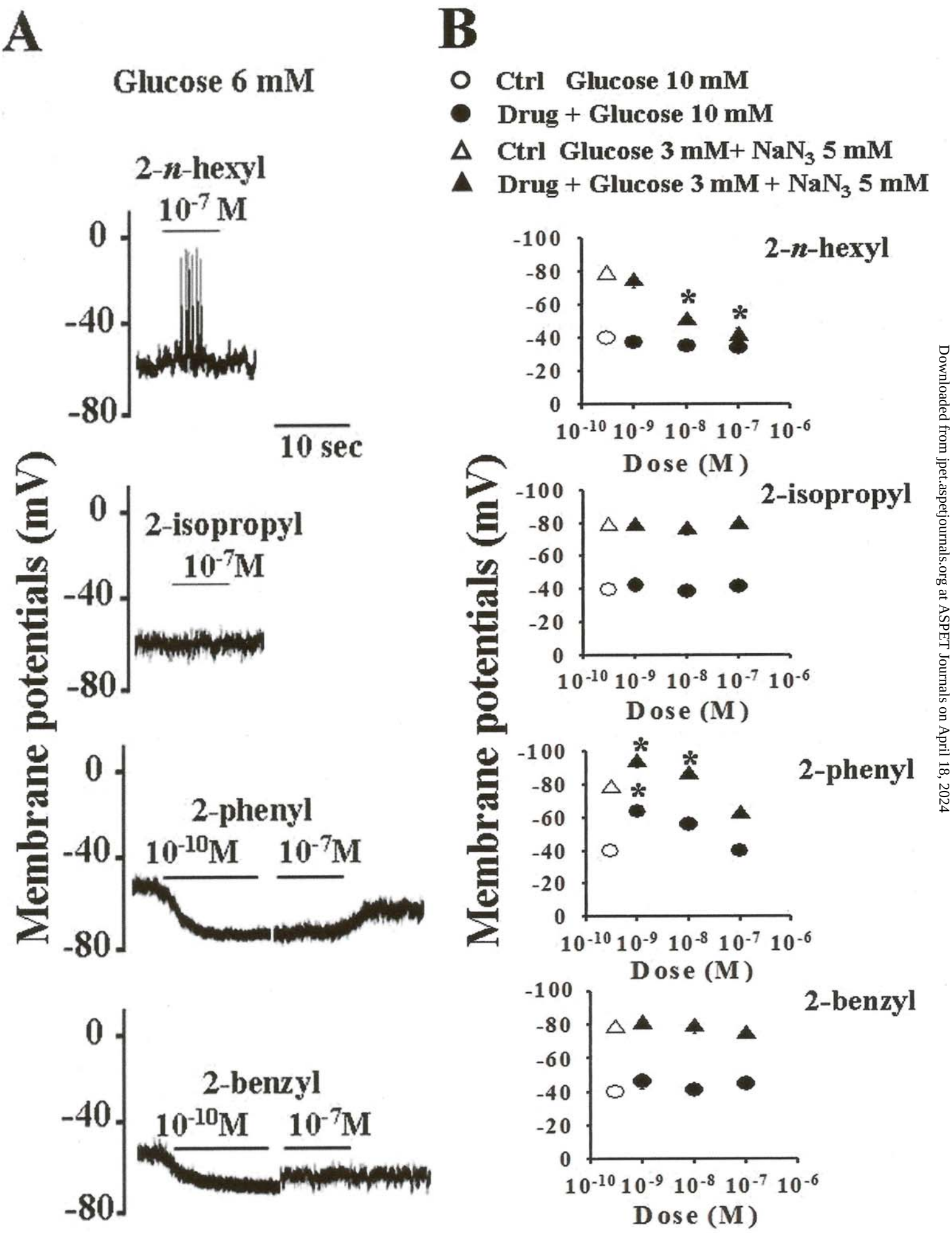

Figure 6

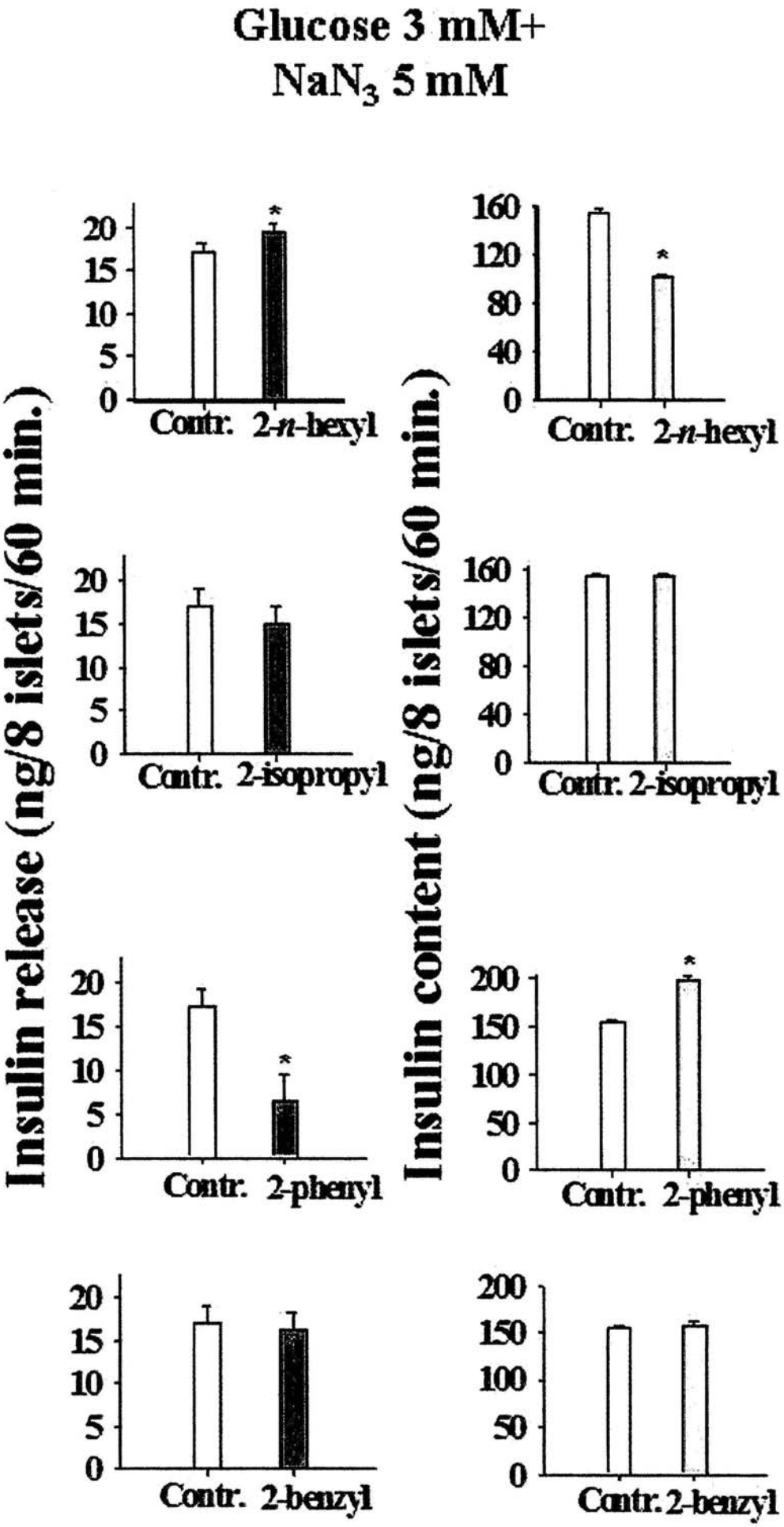

Figure 7

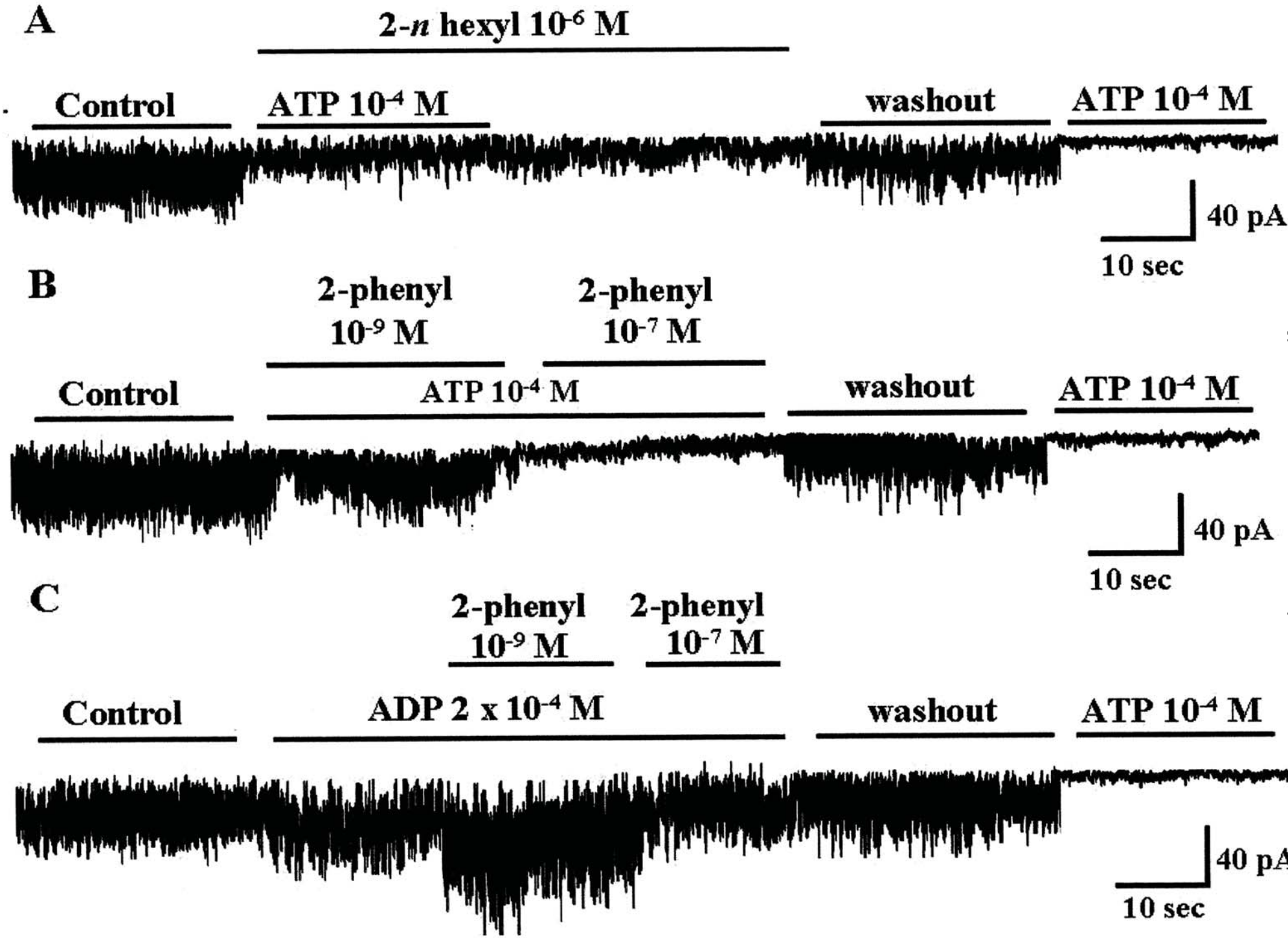

JPET Fast Forward. Published on October 25, 2011 as DOI: 10.1124/jpet.111.185835
This article has not been copyedited and formatted. The final version may differ from this version.

Figure 8

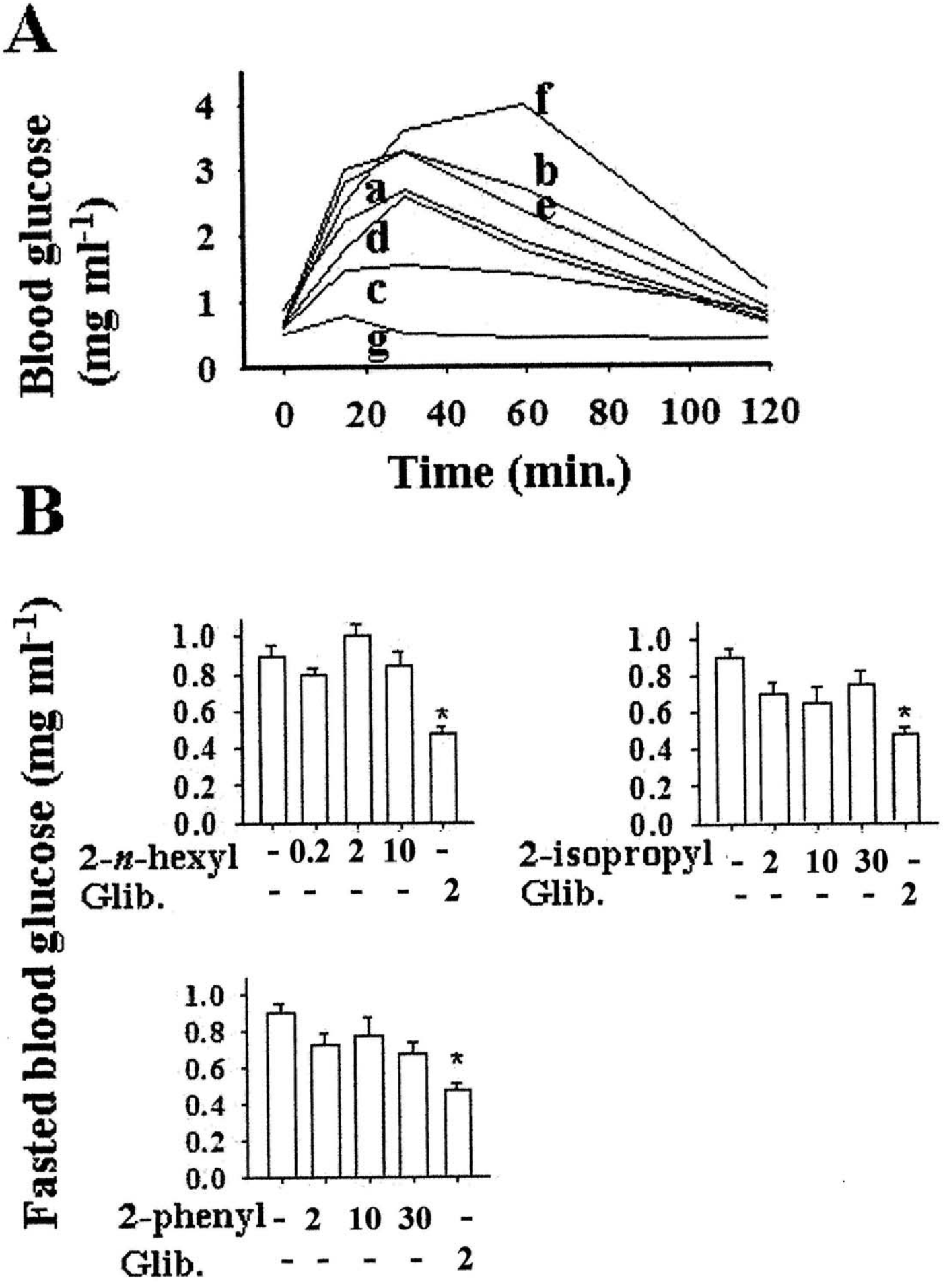

Figure 9